Müller–Stokes Analysis of Long Period Gratings Part II: Randomly Birefringent LPGs

Tinko A. Eftimov, Wojtek J. Bock, *Fellow, IEEE*, Predrag Mikulic, and Jiahua Chen

***Abstract*—We present a Müller–Stokes analysis of the polarization properties of randomly birefingent long-period fiber gratings (LPGs). Using a previously derived Müller matrix, we perform simulations of the polarization behavior in photonic crystal fibers-based tapered long-period gratings with randomly varying birefringence axes. Computer simulations show good agreement with results from experiments with a broadband-amplified spontaneous emission source and a tunable laser in combination with a polarization analyzer.**

***Index Terms*—Müller–Stokes matrix formalism, optical fibers, photonic crystal fibers (PCF), polarization dependent loss (PDL), tapered long-period gratings (TLPG).**

I. Introduction

THE STUDY of polarization properties of long-period fiber gratings (LPGs) and their spectral dependence has basically been restricted to the case of uniform birefringence introduced during their fabrication [1]–[3]. It has been found that LPGs written in even nominally nonbirefringent optical fibers exhibit some birefringence which, independently of the inscription technique, can be subdivided into three types: core birefringence, cladding birefringence, and core-and-cladding birefringence. For the first type, birefringence is in the core and affects only the core mode; for the second it is in the cladding and affects only the higher order cladding modes; and for the third—a combination of the former two [2]. While birefringence has tacitly been considered as uniform, in reality it is random and some results [4] suggest that the total PDL of an LPG is not the sum of individual PDLs of each subsection of the grating. Other studies [5] have identified asymmetric thermal stresses in arc-induced LPGs as the cause of coupling to antisymmetric cladding modes. These asymmetries which are random by nature, however, suggest a possibility for random orientations and strengths of birefringence mechanisms in such types of LPGs. As such parasitic birefringence is undesirable different methods have been proposed to reduce it [6], [7].

Manuscript received February 16, 2008. First published April 21, 2009; current version published August 14, 2009. This work was supportd in part by Natural Sciences and Engineering Research Council of Canada and by the Canada Research Chairs Program.

T. A. Eftimov is with the Faculty of Physics, Plovdiv University, Plovdiv 4000, Bulgaria (e-mail: teftimov@uni-plovdiv.bg).

W. J. Bock is with Canada Research Chair in Photonics with the Université du Québec en Outaouais, Québec, Gatineau J8Y 3X7, Canada (e-mail: Wojtek.Bock@uqo.ca).

J. Chen and P. Mikulic are with the Université du Québec en Outaouais, Québec, Gatineau J8Y 3X7, Canada (e-mail: Jiahua.Chen@uqo.ca; Predrag.Mikulic@uqo.ca).

Digital Object Identifier 10.1109/JLT.2008.2009171

In this part of the present paper, we apply previously derived Mueller matrix for a uniform LPG [8] to perform a theoretical and experimental polarization analysis of randomly birefringent PCF-based LPGs.

Section II is devoted to the application Muller matrix for a uniformly birefringent LPG to such having random orientations of birefringent axes along the periodic structure. The misorientations are represented by a mode-coupling center (MCC). Müller-matrices for random MMCs are used in combination with the matrices derived in Part I of this study to describe an irregular LPG structure.

Section III reports on the experimental study of polarization-dependent properties in arc-induced PCF based LPGs. We first consider the causes of birefringence in LPGs fabricated by arc-induced periodic tapering in an endlessly single-mode (ESM) PCF. Next, we study the spectral dependence of PDL and DOP of PCF tapered LPGs and compare experimental results with computer simulations using the MCC model.

II. Modeling LPGs With Random Birefringence

It has been reported that parasitic birefringence is induced during the fabrication of CO_2-written [2], mechanically impressed [4], and arc-induced LPGs in both SMF-28 [3] and in PCF [8] fibers.

Also, twists of the fiber during tapering are introduced and they lead to rotations of fibre axes. Two basic consequences follow: birefringence varies and birefringence axes randomly change orientation along the LPG structure. We would then have a randomly perturbed birefringent LPG. As the LPG structure is very short, the number of random fluctuations is limited and of the order of the number of pitches. We cannot apply the traditional ensemble averaging technique in this case to derive deterministic equations of polarization transformation along LPGs. The only way to analyze the effects caused by birefringence fluctuations is through simulations. The Müller matrix approach presented in Part I [8] of this study enables us to perform such a simulation using the mode-coupling model [11]. and the corresponding LPG Müller matrices.

We consider the randomly perturbed structure shown in Fig. 2 where we represent the LPG as a series of concatenated birefringent tapers with randomly varying axis orientation.

If the initial polarization at the LPG input is along the x-axis, then this type of perturbation excites partially the Y-polarization in the subsequent tapered region. If the axis has rotated to

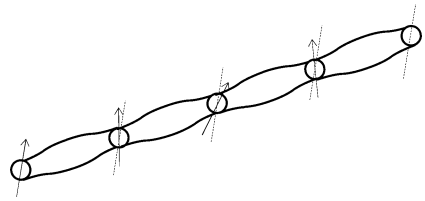

Fig. 1. A tapered LPG with random fluctuations of the birefringence axes.

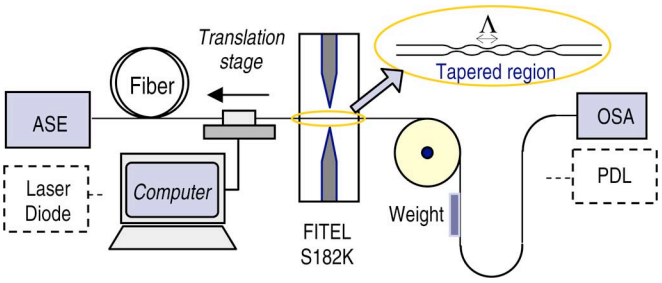

Fig. 2. LPG fabrication setup.

an angle of φ and by letting $\eta = \sin\varphi (\eta = -1 \div 1)$ as the intensity of a mode-coupling coefficient between a X- and a Y-polarization, the Müller matrix is:

$$M_\kappa = \begin{bmatrix} 1 & 0 & 0 & 0 \\ 0 & 1-2\eta^2 & 2\eta\sqrt{1-\eta^2} & 0 \\ 0 & -2\eta\sqrt{1-\eta^2} & 1-2\eta^2 & 0 \\ 0 & 0 & 0 & 1 \end{bmatrix} \quad (1)$$

The Mueller matrix of a mode-coupling center of strength η_i followed by a single taper would be:

$$M_i = M(\Delta z) M_{\eta i} \quad (2)$$

If the LPG consists of n tapers, each randomly shifted to a certain angle, then the resultant Mueller matrix will be:

$$M = M_{\eta n} \cdots M_{\eta i} \cdots M_{\eta 1} M(\Delta z) = \prod_{i=1}^{n} M_{\eta i} M(\Delta z) \quad (3)$$

By generating random numbers for the MCC strengths η_i, we can simulate the effect of random perturbations on the characteristics of the, LPG. Because the number of such MCCs is small we do not assume that their average is zero.

III. Experimental and Simulation Results

We investigated four tapered LPGs fabricated by making use of a FITEL S182K fusion splicer as shown in the arrangement in Fig. 2.

All four LPGs were made from an ESM PCF (ESM-12-01).

The outer shape of a tapered LPG with random fluctuations of the birefringence axes is shown in Fig. 1.

Using the setup shown in Fig. 3, we observe the polarization-dependent spectral transmission responses of the LPGs under test. By rotating the polarizer we find the spectra for which we

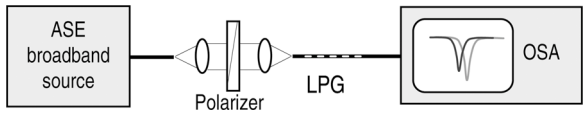

Fig. 3. Experimental setup.

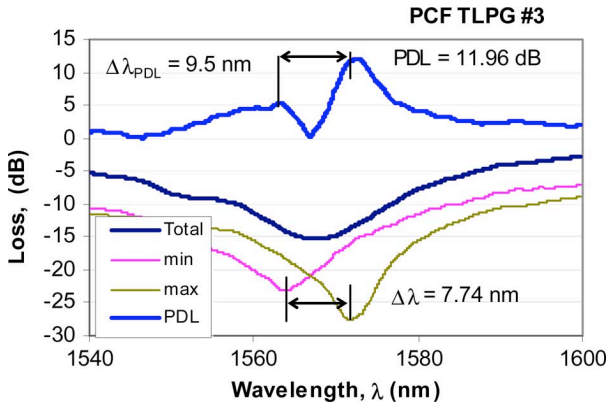

Fig. 4. Polarization dependent spectral response of a PCF tapered LPG.

TABLE I
PDL and Spectral Widths of the PCF LPGS

LPG #	*PDL (dB)*	*Δλ [nm]*	*$\Delta\lambda_{PDL}$ [nm]*
PCF LPG #0	14.19	6.8	14.2
PCF LPG #1	7.5	8.8	17.74
PCF LPG #2	8.17	8.06	11.44
PCF LPG #3	11.96	7.74	9.5

observe a maximum split of the resonance wavelengths $\Delta\lambda = \lambda_{\mathrm{Max}} - \lambda_{\mathrm{min}}$.

Fig. 4 shows the polarization-sensitive responses in a logarithmic scale and the PDL calculated as the difference between the two, which is the same as $10\log(\mathrm{I_x}/\mathrm{I_y})$.

A closer inspection of the curves shows that in contrast to the theoretical calculations [8], the resonance wavelength split as observed from the spectral dependencies of $\mathrm{I_x}$ and $\mathrm{I_y}$ - namely $\Delta\lambda = \lambda_{\mathrm{Max}} - \lambda_{\mathrm{min}}$ - differs from the wavelength separation between the two PDL maxima, which we note as $\Delta\lambda_{\mathrm{PDL}}$. We thus have $\Delta\lambda < \Delta\lambda_{\mathrm{PDL}}$.

This inequality is observed for all tested samples as is evident from the summary presented in Table I.

Furthermore, the PDL curve is asymmetric.

As commented in Part I, we assume that these discrepancies are caused by the presence of random birefringence in the LPG under test.

To verify this assumption, we cut TLPGs at the points of minimum and maximum diameters and observed the cross sections with a Hitachi scanning electron microscope (SEM). The same was done on a pristine PCF from which the TLPGs were manufactured.

For each cross section, we determine the ellipticity of each hole, its orientation and form an ellipticity vector $\mathbf{e_i}$.

The effective ellipticity and effective orientation angle is then calculated for each hexagonal ring of holes around the core using (28) and (29) from Part I [8].

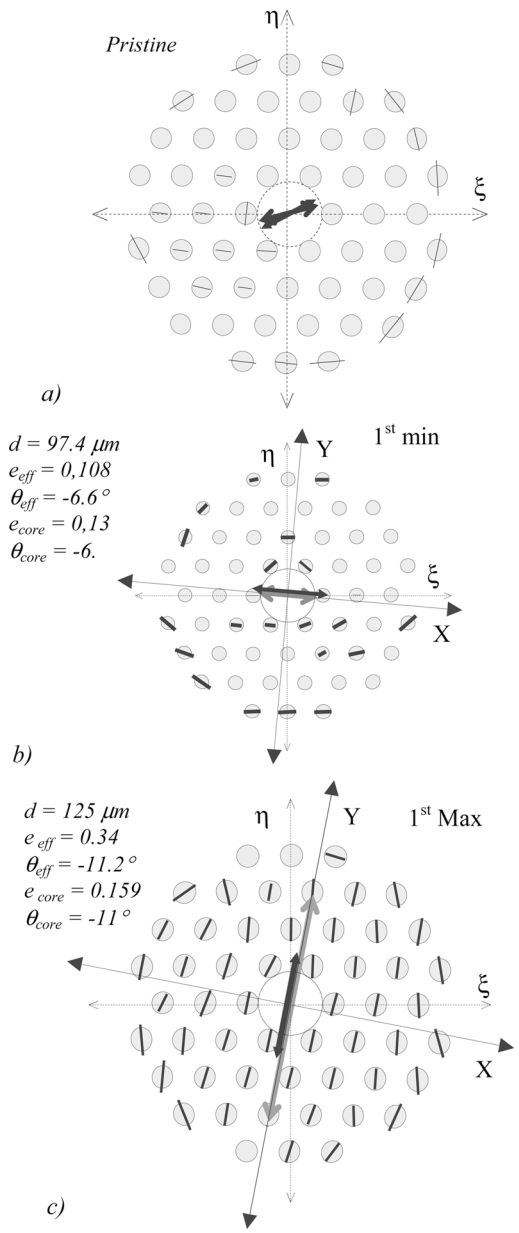

Fig. 5. Shapes of the holes in a tapered PCF-based LPG: (a) the pristine fiber; (b) across a section of the LPG with a minimum diameter; (c) across a section of the LPG with a maximum diameter.

TABLE II
ELLIPTICITIES AND ORIENTATIONS AT DIFFERENT POINTS ALONG PCF LPGS

Fiber section	d [μm]	e_{eff}	θ_{eff} [°]	e_{core}	θ_{core} [°]
Pristine	125	0	15	≈ 0	28
1st min	97.4	0.108	-6.6	0.13	6
-					
1st max	125	0.34	-11.2	0.159	-11
2nd min	96.6	0.4	1.37	0.28	91
2nd max	125	0.357	12.6	0.12	15

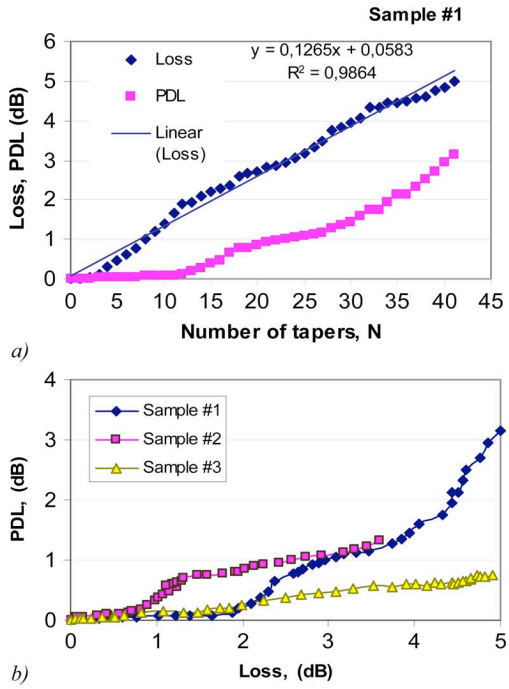

Fig. 6. Loss and PDL in PCF based LPGs: (a) dependences on the number of tapers; (b) PDL versus total loss.

For the sake of simplicity we perform the sum over all the holes in the cross section. Fig. 5(a) shows the results for the pristine PCF, while Figs. 5(b) and (c) show the individual and effective ellipticities for the holes and for the core region for sections of minimum and maximum diameter.

Indicated are the corresponding ellipticity vectors for the core and for the cladding.

As is clearly seen, the effective ellipticity vectors do not coincide with the ξ, η local axis and the angle θ_{eff} as well as e_{eff} vary from section to section as is summarized in Table II.

Although the number of cross sections studied is limited it is clear that the birefringence axis fluctuations are considerable and reach as much as 13° in either directions.

As this would lead to cross-polarization coupling, then in combination with the PDL loss in an ideal birefringent LPG we should expect large variations of the PDL from one TLPG to another. The reason for these large variations is due to the fact that the number of tapers n in a LPG is of the order of 20–40 which is insufficient to achieve averaging over all possible angle fluctuations. Also, this means that the dependence of the PDL on the total loss along a TLPG will be nonlinear in the general case, because while general losses add up arithmetically in dB units, polarization dependent losses do not, since in the general case the PDL can be represented as a vector [9], [10].

To verify this conclusion we applied the fabrication procedure to a section of a PCF fiber and measured both the total losses and the PDL after each subsequent taper. The setup of Fig. 2 was used with a 1550 nm laser diode and a JDSUniphase PS3 PDL multimeter, both shown in broken lines.

We tested three samples and the results are presented in Fig. 6(a), (b). Fig. 6(a) shows the evolution of the total losses and the PDL with the number of tapers during the process of TLPG formation for the first of the three samples tested. It is seen that generally the total losses tend to increase linearly with the number of tapers. However the evolution of the PDL is definitely not linear as concluded previously. Fig. 6(b) presents the PDL versus loss dependencies for all of the three samples

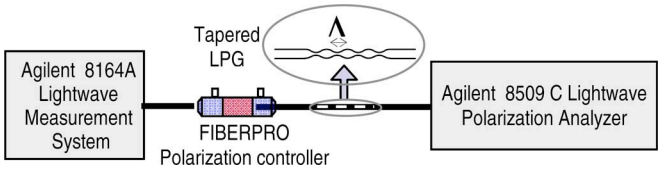

Fig. 7. Experimental setup used for the measurement of the wavelength dependence of the Stokes parameters and the DOP.

under test. What we see is that there are large individual fluctuations from sample to sample. However, it was noticed that PDL initially changes very little until the first ten tapers and then starts increasing at a greater rate exhibiting several stages of growth. It was also found out that during the tapering the fiber structure was rotating. This rotation was easily observable on the splicer screen for a PCF fiber because the parallel holes are visible and any rotation is detectable, though the rotation angle is not directly measurable.

We believe similar mechanisms are at work during the formation of SMF-28 based tapered LPGs. We note that our simulation results from Fig. 6(b) follow similar dependence as the PDL versus Loss reported by [4]. Having thus identified a major cause for the birefringence and PDL fluctuations caused by the specific fabrication process we further proceed to simulate their effect on the polarization properties of the TLPG.

To study the polarization properties of birefringent TLPGs in greater detail we use the experimental setup shown in Fig. 7.

The source in this case is a tunable laser, with a degree of polarization close to 100%. The output state of polarization is measured using Agilent 8509C polarization analyzer, which measures the individual Stokes parameters and plots the evolution of polarization on a Poincaré sphere. The FiberPro polarization controller was used to change the state of polarization at the TLPG input. Unfortunately, there is no way to determine what the actual state of polarization at the TLPG input is. What the polarimeter "sees" is the state of polarization after the fibers leading out of the TLPG. We have changed the input state of polarization and observed the wavelength dependence of the Stokes parameters. First a test without a TLPG was carried out and it was found that the state of polarization did not change on the Poincaré sphere. It was found out that the state of polarization was dependent on the wavelength and on the initial state of polarization at the grating input. Figs. 8(a)–(c)) show the spectral dependence of the total power, of the X- and Y-polarized intensities (at the polarimeter!) and of the PDL, calculated as $\mathrm{PDL} = 10.\log[(S_0 + S_1)(/(S_0 - S_1)]$. Strictly speaking this formula is true only for a depolarized input and for a fully polarized elliptical input it is a pseudo-PDL since it is not calculated from the general formula (17–18).

To use the general formula we have to know the exact Mueller matrix of a randomly perturbed TLPG, which we do not. It is however a good indicator of PDL associated properties especially with equal polarization excitation. The Stokes parameters in the inset of Fig. 8(a) refer to the lowest wavelength of the spectral scan and represent the initial vector $\mathbf{S}^\circ$ from Fig. 9(a). The Stokes parameters in Fig. 8(b) have the same meaning and represent the initial vector from Fig. 9(b) which is orthogonal to $\mathbf{S}^\circ$. These two cases were obtained for different settings of the

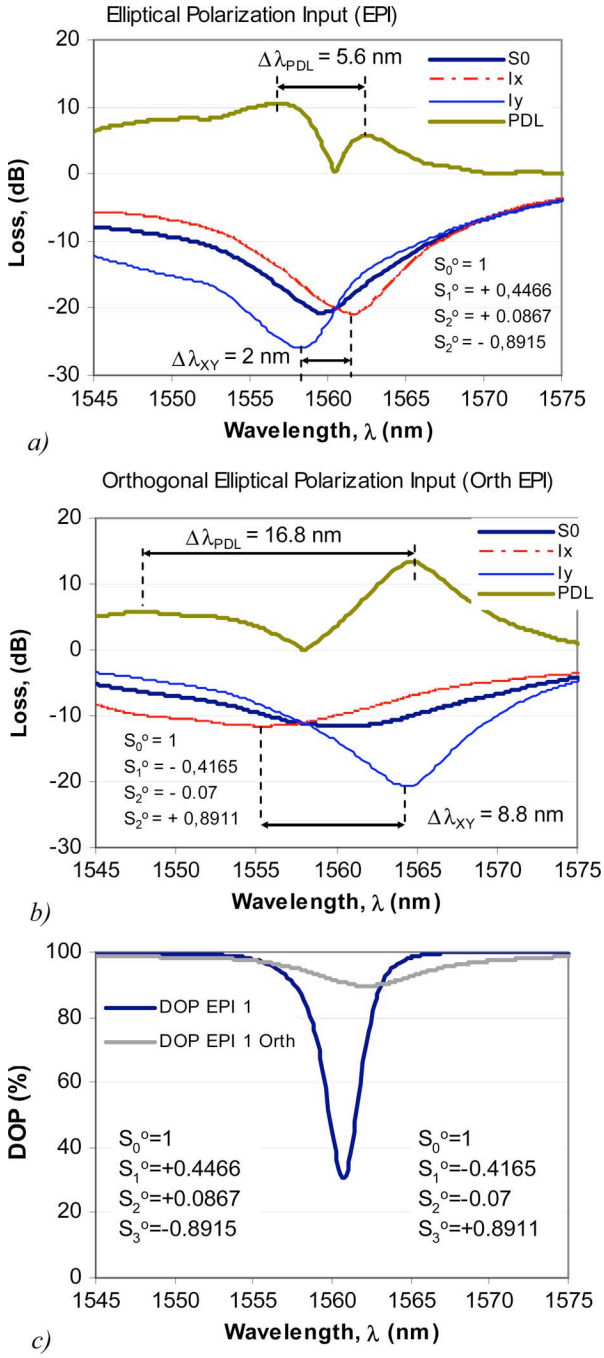

Fig. 8. Spectral evolution of the state of polarization with for a PCF based LPG for two almost orthogonal states of polarization: (a) Losses and PDL for an elliptical polarization input; (b) Losses and PDL for an orthogonal elliptical state of polarization; (c) DoP for the two mutually orthogonal elliptical input states of polarization.

polarization controller. Fig. 8(c)) shows a comparison between the measured DOPs for these two cases. It should be noted that mutually orthogonal polarizations at the TLPG output does not infer mutually orthogonal polarization states at the TLPG input. Rather, they would be close to orthogonal. The general comparison with the theoretically calculated spectral plots of the I_x, I_y, the total power, the PDL and the DOP shows the following features. First, the curves are not symmetrical any more as in the ideal case. Second, the DOP shows a single minimum and the

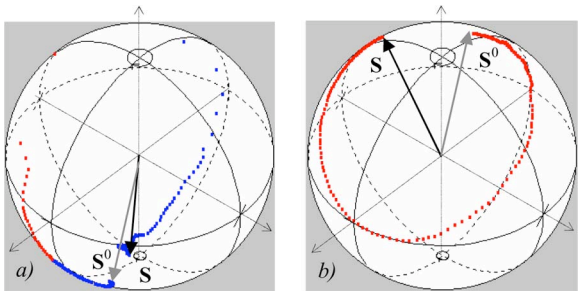

Fig. 9. Evolution of the polarization on the Poincaré sphere in the LPG for the measurements shown in Fig. 12(a) and (b).

fine structure of the central maximum is lost. Third, the wavelength split between the I_x and I_y minima is smaller than that between the PDL maxima i.e., $\Delta\lambda < \Delta\lambda_{\mathrm{PDL}}$

As we assume that these deviations from the ideal birefringent LPG are due to the random fluctuations of the birefringence axes, we can resort to some simulation following the procedure described in Section II.

We first must note that since the number of tapers is too small $(\mathrm{n} < 40)$ the number of MCCs is small, too. No ensemble averaging is possible so large variations are to be expected depending on the strength and sign of the MCCs.

As we have observed that the birefringence axis may vary as much as $\pm 13^{\circ}$ this implies that $|\eta| < 0,22$. We do not impose any condition on the average strength of the MCCs generated. To simplify the simulations only four mode coupling centers with strengths $\eta_1 = -0.11, \eta_2 = -0.16, \eta_3 = -0.11$, and $\eta_4 = 0.1$ were used for a TLPG of parameters considered above.

In Figs. 10(a)–(c)) we show the plots from a simulation of the wavelength dependence of I_x, I_y, S_0, the PDL and the DOP for two mutually orthogonal polarizations whose Stokes parameters at the TLPG input are $\mathbf{S}_0 = (1, -0.9846, 0.0517, 0.0896, 0)$ and $\mathbf{S}_{0\perp} = (1, 0.9846, -0.0517, -0.0896, 0)$ for an input $\mathrm{DOP}_0 = 0.99$.

The curves show the same as in the experimental results from Figs. 8 and 9. Unlike the experimental data where we could not exactly set two orthogonal polarization states at TLPG's input, in the computational experiment we can and we find that mutually orthogonal polarization inputs do not lead to symmetric results as in the case of uniformly birefringent LPG as is evident from Fig. 10. We also find out that in the computer simulation, as in the real case $\Delta\lambda \neq \Delta\lambda_{\mathrm{PDL}} \neq \Delta\lambda_{\mathrm{DOP}}$. Although, for the sake of simplicity, in the simulation we have taken into account only fluctuations of the birefringence axes orientation we see that the basic distortions from the ideal case observed in real experiment are well described and confirm our conclusions about the nature of birefringence in tapered PCF-based LPGs.

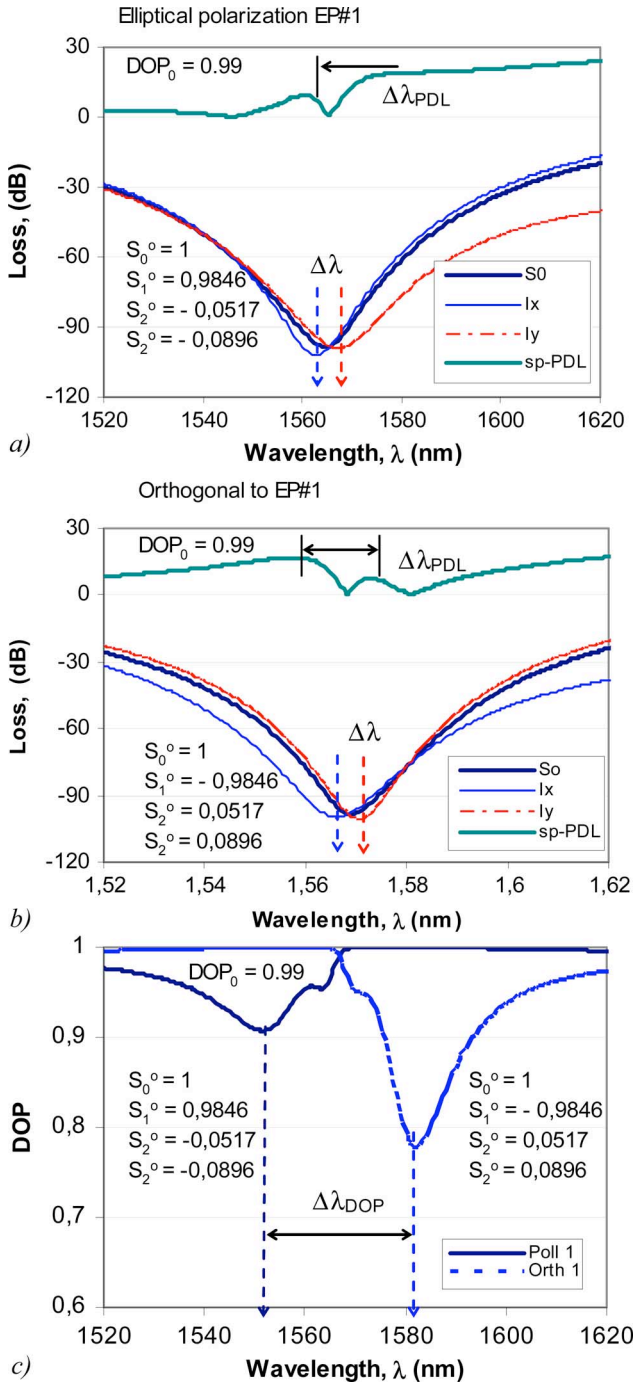

Fig. 10. Simulation of the spectral evolution of the state of polarization with for a PCF based LPG for two almost orthogonal states of polarization: (a) Losses and PDL for an elliptical polarization input; (b) Losses and PDL for an orthogonal elliptical state of polarization; (c) DOP for the two mutually orthogonal elliptical input states of polarization.

IV. Conclusion

We have performed a detailed Müller–Stokes analysis of the polarization properties of LPGs with random birefringence which is supported by experimental results from PCF-based tapered LPGs.

Using the Müller transfer matrix of a uniformly birefringent LPG in combination with mode coupling center model we performed computer simulation of the polarization properties of LPGs with random birefringence which show good agreement with the experimental data obtained.

The growth of resultant PDL for an LPG was compared to that of the total losses and the nonlinear dependence reveled the random orientations of the PDL vector of each tapered section. The presence of random birefringence was found to cause asymmetries in the PDL as well as in the DOP for orthogonal polarization excitations and different resonance wavelength splits in

the spectral dependences of the PDL, the DOP and polarized intensity curves.

ACKNOWLEDGMENT

The authors gratefully acknowledge support for this work by the Natural Sciences and Engineering Research Council of Canada and by the Canada Research Chair Program.

REFERENCES

[1] Y. Zhu, E. Simova, P. Berin, and C. Grover, "A comparison of wavelength-dependent polarization-dependent loss measurements in fiber gratings," *IEEE Trans. Instrum. Meas.*, vol. 49, pp. 1231–1239, 2000.

[2] B. L. Bachim and T. K. Gaylord, "Polarization-dependent loss and birefringence in long-period fiber gratings," *Appl. Opt.*, vol. 42, pp. 6816–6823, 2003.

[3] G. M. Rego, J. L. Santos, and H. M. Salgado, "Polarization-dependent loss of arc-induced long-period gratings," *Opt. Commun.*, vol. 262, pp. 152–156, 2006.

[4] G. Rego, M. Morais, J. L. Santos, and H. M. Salgado, "PDL and DGD measurements of mechanically induced long-period fiber gratings," in *Commun. Symp.*, London, 2003, pp. 77–80 [Online]. Available: http://www.ee.ucl.ac.uk/lcs/papers2003/index.html, Available

[5] O. V. Ivanov and G. M. Rego, "Origin of coupling to antisymmetric modes in arc-induced long-period fiber gratings," *Opt. Exp.* vol. 15, pp. 13936–13941, 2007 [Online]. Available: http://www.opticsinfobase.org/abstract.cfm?URI=oe-15-21-13936, Available

[6] S. T. Oh, W. T. Han, U. C. Paek, and Y. Chung, "Reduction of birefringence and polarization-dependent loss of long-period fiber gratings fabricated with a KrF excimer laser," *Opt. Exp.* vol. 11, pp. 3087–3092, 2003 [Online]. Available: http://www.opticsinfobase.org/abstract.cfm?URI=oe-11-23-3087, Available

[7] S. T. Oh, W. T. Han, U. C. Paek, and Y. Chung, "Azimuthally symmetric long-period fiber gratings fabricated with CO_2 laser," *Microw. Opt. Technol. Lett.*, vol. 41, pp. 188–190, 2004.

[8] T. Eftimov, W. Bock, J. Chen, and P. Mikulic, "Mueller matrix analysis of long period gratrings. Part I: uniformly birefringetn LPGs," *J. Lightw. Technol.*, submitted for publication.

[9] N. Gisin, "Statistics of polarization-dependent losses," *Opt. Commun.*, vol. 114, pp. 399–40, 1995.

[10] T. Eftimov, "Müller matrix analysis of PDL components," *Fiber and Integrated Optics*, vol. 23, pp. 453–466, 2004.

[11] J. Olszewski, T. Nasilowski, M. Szpulak, G. Sttkiewicz, T. Martynkinen, W. Urbanczyk, J. Wojcik, P. Mergo, M. Makara, F. Berghmans, and H. Thienpont, "Analysis of birefringent doped-core holey fibers for Bragg gratings," in *Proc. SPIE OFS-17*, Belgium, 2005, vol. 1, pp. 351–354.

Tinko A. Eftimov was born in Bulgaria, 1955. He received the M.S. degree in quantum electronics from the Sofia University, Sofia, Bulgaria, in 1982 and the Ph.D. degree in applied physics from the Technical University, Sofia, Bulgaria, in 1989.

He is currently with the Department of Experimental Physics, Plovdiv University, Bulgaria. His interests include optical fibers, polarization phenomena, intermodal interference, fiber gratings and fiber optic sensors. In these fields he has authored and co-authored more than 60 journal and conference papers.

Wojtek J. Bock (M'85–SM'90–F'03) received the M.Sc. degree in electrical engineering and the Ph.D. degree in solid state physics from the Warsaw University of Technology, Poland, in 1971 and 1980, respectively.

He is currently a Full Professor of Electrical Engineering and Canada Research Chair in Photonics at the Université du Québec en Outaouais, Canada. He is also Director of the Photonics Research Center at this University. His research interests include fiber optic sensors and devices, multisensor systems, and precise measurement systems of non electric quantities. He has authored and coauthored more than 240 scientific papers, patents and conference papers in the fields of fiber optics and metrology.

Dr. Bock is a Fellow of IEEE and for eight years was a member of the Administrative Committee of the IEEE Instrumentation and Measurement Society. In May 1997 he was General Chairman of the IMTC/97 in Ottawa, Canada.

Predrag Mikulic received the Associate of Science degree as a Telecommunication Engineering Technologist from the University of Sarajevo, Sarajevo, Yugoslavia, in 1989.

He is currently with the Centre de Recherche en Photonique, Université du Québec en Outaouais, Gatineau, QC, Canada. His current research interests include thin films depositions, excimer lasers, photonic devices, fiber sensors, splicing procedures of dissimilar fibers including photonic crystal fibers.

Jiahua Chen graduated from the Precision Instrument Department, Tsinghua University, Beijing, China in 1970.

He is now in the Centre de recherche en Photonique, Département d'informatique et d'ingénierie, Université du Québec en Outaouais, Québec, Canada. His interests include optical fibers, polarization phenomena, fiber gratings, and optical fiber pressure sensors.